



Thermal-mechanical and springback behavior of dual-phase steel at warm temperatures

LIN Qi-quan(林启权)¹, WANG Zhen-zhu(王镇柱)¹, DONG Wen-zheng(董文正)^{1,2*},
BU Gen(卜根)¹, HUANG Jin-shan(黄巾珊)¹

1. School of Mechanical Engineering, Xiangtan University, Xiangtan 411105, China;
2. Department of Mechanical and Systems Engineering, Gifu University, Yanagido 501-1193, Japan

© Central South University 2022

Abstract: For non-quenchable dual-phase (DP) steel sheet, the warm forming process can effectively reduce the amount of springback, and the mechanical parameters that influence its elastic and inelastic recovery to decrease exhibit a strong temperature dependence, especially under cyclic loading conditions. In this paper, the monotonic and cyclic loading tests of DP980 steel sheets are conducted at the temperatures ranging from 25 °C to 500 °C. The temperature-dependent flow stress, nonlinear elastic recovery, and Bauschinger effect are investigated. The results demonstrate that both the elastic modulus and Bauschinger effect show an exponential law with pre-strain, and decrease with the increase of forming temperature, while there will be an abnormal phenomenon of rebound due to the influence of dynamic strain aging effect. Meanwhile, a linear relationship between the Bauschinger effect and inelastic strain is observed at various temperatures, and the weight of the Bauschinger effect in the total strain reduces with temperature increasing, which indicates that the springback is dominated by linear elastic recovery. Furthermore, the U-draw bending tests are carried out to clarify the influence of Vickers hardness distribution and martensite size effect on the springback behavior.

Key words: warm forming; dual-phase steel; springback behavior; nonlinear elastic recovery; Bauschinger effect

Cite this article as: LIN Qi-quan, WANG Zhen-zhu, DONG Wen-zheng, BU Gen, HUANG Jin-shan. Thermal-mechanical and springback behavior of dual-phase steel at warm temperatures [J]. Journal of Central South University, 2022, 29(6): 1895–1905. DOI: <https://doi.org/10.1007/s11771-022-5042-5>.

1 Introduction

Energy-saving and lightweight are the eternal themes in the automobile manufacturing industry. For one thing, various new processes, such as plate forging [1–2], have been developed to form a complicated and functional part. For another, dual-phase (DP) steel is widely used in the body-in-white (BIW) components due to its good formability, high strength, and considerable cost. Dual-phase steel

consists of hard martensite (M) islands embedded in a soft ferrite phase (F), and its strength increases with the increase of martensite proportion. However, it brings more challenges to the forming process with the increasing strength of DP steel, among which the significant springback is one of the critical issues to be solved.

Hot-stamping is the most popular forming technology to obtain small or no springback parts at present [3–4], but it is not suitable for forming DP steel which does not have sufficient hardenability. It

Foundation item: Projects(2020JJ4578, 2019JJ50604) supported by the Natural Science Foundation of Hunan Province, China; Project (19A499) supported by the Key Program of the Scientific Research Foundation of the Education Department of Hunan Province, China

Received date: 2021-02-04; **Accepted date:** 2021-09-20

Corresponding author: DONG Wen-zheng, PhD, Associate Professor; Tel: +86-731-58292209; E-mail: wzdong@xtu.edu.cn; ORCID: <https://orcid.org/0000-0001-5516-2558>

is worth to mention that warm forming can effectively reduce the springback of non-quenchable advanced high strength steels [5]. LEE et al [6] proposed a local heating method by near-infrared rays in V-bending and 2D-draw bending to reduce the springback of DP980. At the same time, they used the rate-independent Johnson-Cook model to accurately predict the springback. This is one of the few cases where the springback prediction is extraordinarily accurate without considering the nonlinear elasticity and Bauschinger effect. SAITO et al [7] investigated the warm forming of 980 MPa nano-precipitation strengthened steel. It was pointed out that the main reason for springback reduction during warm forming is the stress softening, residual stress reduction, and unloading creep caused by elevated temperature. OZTURK et al [8] studied the springback behavior of DP600 at the temperatures ranging from room temperature to 300 °C during isothermal forming. It was concluded that heating and forming in the furnace will reduce springback, but high temperature will reduce the elongation and formability of dual-phase steel. KAYHAN et al [9] found that the limit drawing ratio of DP600 steel sheet increases with the increase of temperature during non-isothermal forming. MORI et al [10] used the resistance heating method to study the formability of SPFC 980 steel sheet in the temperature range from room temperature to 800 °C. The results showed that the springback decreased obviously with the increase of temperature, and the elongation and thinning rate were also improved. Therefore, warming forming is suitable for dual-phase steel to reduce the springback. The temperature-dependent behavior of dual-phase steel should be analyzed in depth to minimize the springback and ensure its good formability.

The present work aims to investigate the temperature-dependent evolution of nonlinear elastic recovery and the Bauschinger effect and its contribution to springback during warm forming. The monotonic tensile tests, uniaxial loading-unloading-reloading (ULUR) tests, and U-draw bending tests are conducted at different temperatures. The temperature dependence of flow stress, elastic modulus, Bauschinger effect loop width, and Bauschinger effect loop area are

observed and discussed. Furthermore, the microstructure and the hardness of U-shape parts at special position related to springback are also examined.

2 Experimental methods

2.1 Mechanical tests

The isothermal uniaxial loading tests were conducted at 25, 100, 200, 300, 400 and 500 °C in the MTS 810 material test system equipped with a high-temperature furnace. The DP980 steel sheet had a thickness of 1.2 mm. The specimens as shown in Figure 1(a) were prepared, along the rolling direction. Each specimen was heated to the target temperature and held for 10 min, and a constant crosshead speed of 3 mm/min was adopted during the test.

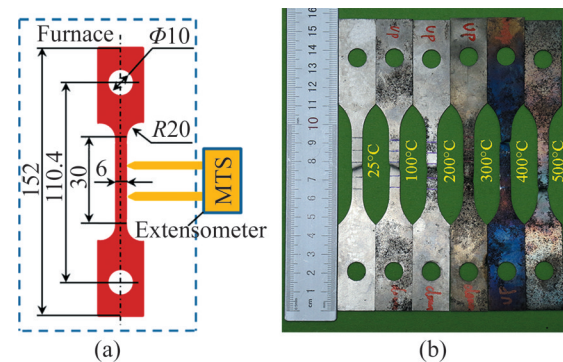


Figure 1 (a) Schematic of uniaxial loading tests and ULUR tests; (b) Example of specimen for uniaxial loading tests at elevated temperature (Unit: mm)

The isothermal ULUR tensile tests were carried out using the same specimen as the uniaxial loading tests, while the temperatures ranging from 25 to 400 °C were used since the elongation decreased significantly at 500 °C. During the loading phase, the displacement-control method was adopted to stretch the specimen to the target pre-strain level. As for the unloading phase, the force-control method was used to achieve the nearly complete unloading [11]. To reduce the experimental error caused by the unloading force of the clamp, the force at the end of unloading phase was set to 5 N. This incomplete unloading procedure to obtain the elastic modulus used for predicting springback has been reported by ZANG et al [12].

2.2 U-draw bending tests

U-draw bending tests along the rolling direction were carried out under non-isothermal conditions. The tools and process parameters are shown in Figure 2. During the whole stamping process, a blank sheet with a width of 20 mm and a length of 120 mm, was heated to the target temperature for no less than 10 min, and then rapidly transferred to the mold in less than 7 s. Subsequently, the punch contacted the blank sheet and moved 35 mm. After unloading, the springback behavior of U-shape parts could be observed.

To clarify the influence of the microstructure on springback, the Vickers hardness and martensite area fraction of the U-shape parts at various heating temperatures were analyzed. The Vickers hardness along the U-shape profile was measured at a load of 3.0 N. The samples for microstructure characterization were ground, polished, and then etched with 4.0% nitric acid alcohol solution. The martensite morphology was observed using a scanning electron microscope (SEM).

3 Results and discussion

3.1 Thermal-mechanical behavior

3.1.1 Temperature dependence of stress–strain response

To investigate the influencing mechanism of elastic and inelastic recovery behavior on springback during warm forming, the temperature-dependent flow stress, elastic modulus, Bauschinger effect, and hardness distribution are examined.

The springback angular is larger with a higher stress level during unloading [13]. Figure 3(a) shows that the flow stress and the yield stress decrease significantly with the temperature increasing from 25 °C to 500 °C. In particular, the flow stress just fluctuates slightly with the increasing temperature when the temperature is in the range of 100–300 °C and the strain is lower than 0.03, while the flow stress curves intersect at the strain of 0.03 and 0.07 respectively. In order to clarify the small fluctuations and intersections of

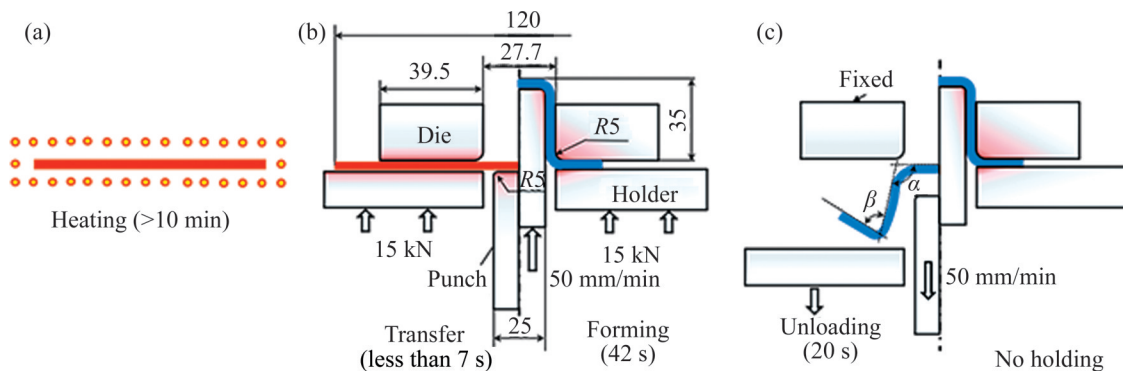


Figure 2 Schematic diagram of non-isothermal warm forming process: (a) Heating process; (b) Forming process (unit: mm); (c) Unloading process

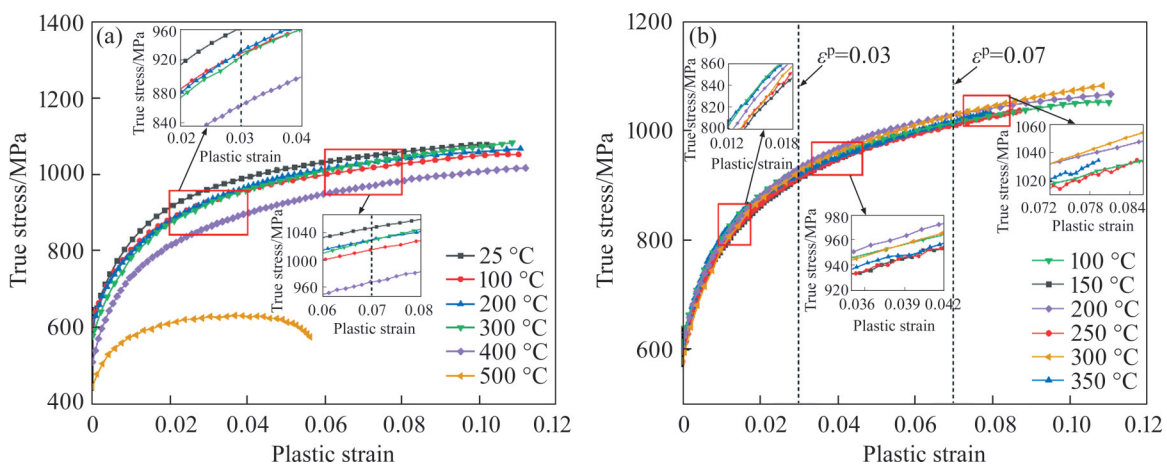


Figure 3 True stress–strain curves of monotonic loading test along rolling direction: (a) $T=25, 100, 200, 300, 400$ and 500 °C; (b) $T=100, 150, 200, 250, 300$ and 350 °C

flow stress, the flow stress curves in the temperature range of 100 – 350 °C are analyzed in detail, as shown in Figure 3(b).

According to Figure 3(b), the flow stress of DP980 also shows an unusual rise-and-down tendency as the temperature increases. When the strain is below 0.03, the flow stress curves can be sorted from the highest to the lowest stress as $T=100, 350, 200, 300, 250$ and 150 °C. The sequence of the flow stress curve is shifted when the strain is between 0.03 and 0.07, when $T=200, 300, 100, 350, 150$ and 250 °C, respectively. As the strain is greater than 0.07, the order of the flow stress curves

changes again, as $T=300, 200, 350, 100, 150$ and 250 °C, respectively. These results indicate that the DP980 steel sheet has no obvious thermal-softening behavior in the temperature range. In addition, it has a significant temperature-dependent hardening rate during the whole stage of plastic deformation. A similar trend for DP590 steel sheet was also reported by CAI et al [14]. It points out that these abnormal behaviors are caused by the high bake hardening properties of the dual-phase steel.

The true stress–strain response of ULUR tests at elevated temperature is illustrated in Figure 4. It shows that the stress–strain curves after cyclic re-

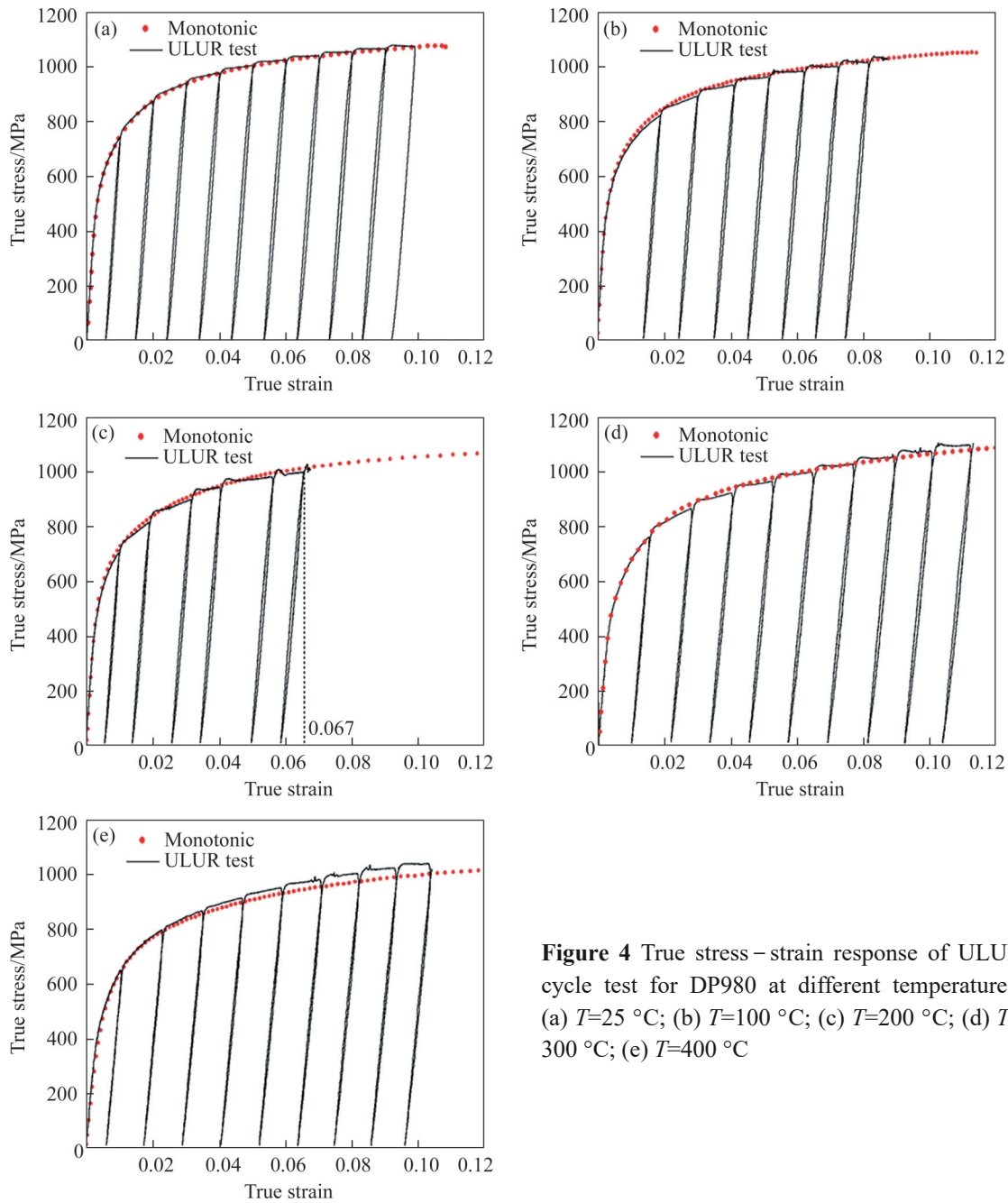


Figure 4 True stress–strain response of ULUR cycle test for DP980 at different temperatures: (a) $T=25$ °C; (b) $T=100$ °C; (c) $T=200$ °C; (d) $T=300$ °C; (e) $T=400$ °C

yield at $T=25\text{ }^{\circ}\text{C}$, $100\text{ }^{\circ}\text{C}$, $200\text{ }^{\circ}\text{C}$ are almost the same as the monotonic loading curves, while the cyclic stress at large strain is slightly higher than the monotonic stress after $T=300\text{ }^{\circ}\text{C}$, which indicates that a slight cyclic hardening behavior is observed in DP980 steel sheet as the temperature increases. Furthermore, the elongation of the ULUR tests is lower than that of the monotonic test, especially at $T=100\text{ }^{\circ}\text{C}$ and $200\text{ }^{\circ}\text{C}$. This may be caused by the cyclic fatigue and fracture effects of the DP980 steel sheet, and these effects are more significant at $T=100\text{ }^{\circ}\text{C}$ and $200\text{ }^{\circ}\text{C}$.

3.1.2 Temperature dependence of elastic modulus

To minimize the inevitable noise of the tensile machine during the test, the initial elastic modulus is obtained by using the linear regression method via fitting the stress data from 50 MPa up to half of the yield stress, as shown in Figure 5(a) [15]. From Figure 5(a), the chord modulus E_{chord} is the secant to the unloading and reloading curves, which is widely used to predict springback since it can be easily implemented in finite element through a simple

code. The ε_e and ε_{in} represent the pure elastic strain and inelastic strain, respectively. The ε_e is recoverable and energy-conserving, while the ε_{in} is recoverable and energy-dissipating [16].

Figure 5(b) shows that the ratio of inelastic strain to elastic strain increases with the increase of pre-strain at each temperature. A significant temperature-dependence of this ratio can be observed. The ratio of $\varepsilon_{in}/\varepsilon_e$ at $T=200\text{ }^{\circ}\text{C}$ is lower than that at $T=25\text{ }^{\circ}\text{C}$, $100\text{ }^{\circ}\text{C}$ and $300\text{ }^{\circ}\text{C}$. With the inelastic strain at large pre-strain being only 10% of the elastic strain, the value of $\varepsilon_{in}/\varepsilon_e$ is the lowest at $T=400\text{ }^{\circ}\text{C}$, which suggests that the degree of inelastic strain in the total strain recovery is gradually weakened, and the elastic recovery is mainly linear elasticity. Furthermore, the ratio of $\varepsilon_{in}/\varepsilon_e$ at $T=300\text{ }^{\circ}\text{C}$ is higher than that at $T=200\text{ }^{\circ}\text{C}$, which may result from the dynamic strain aging effect having a significant influence on the inelastic strain at these temperatures [17].

Figure 5(c) shows that the chord elastic

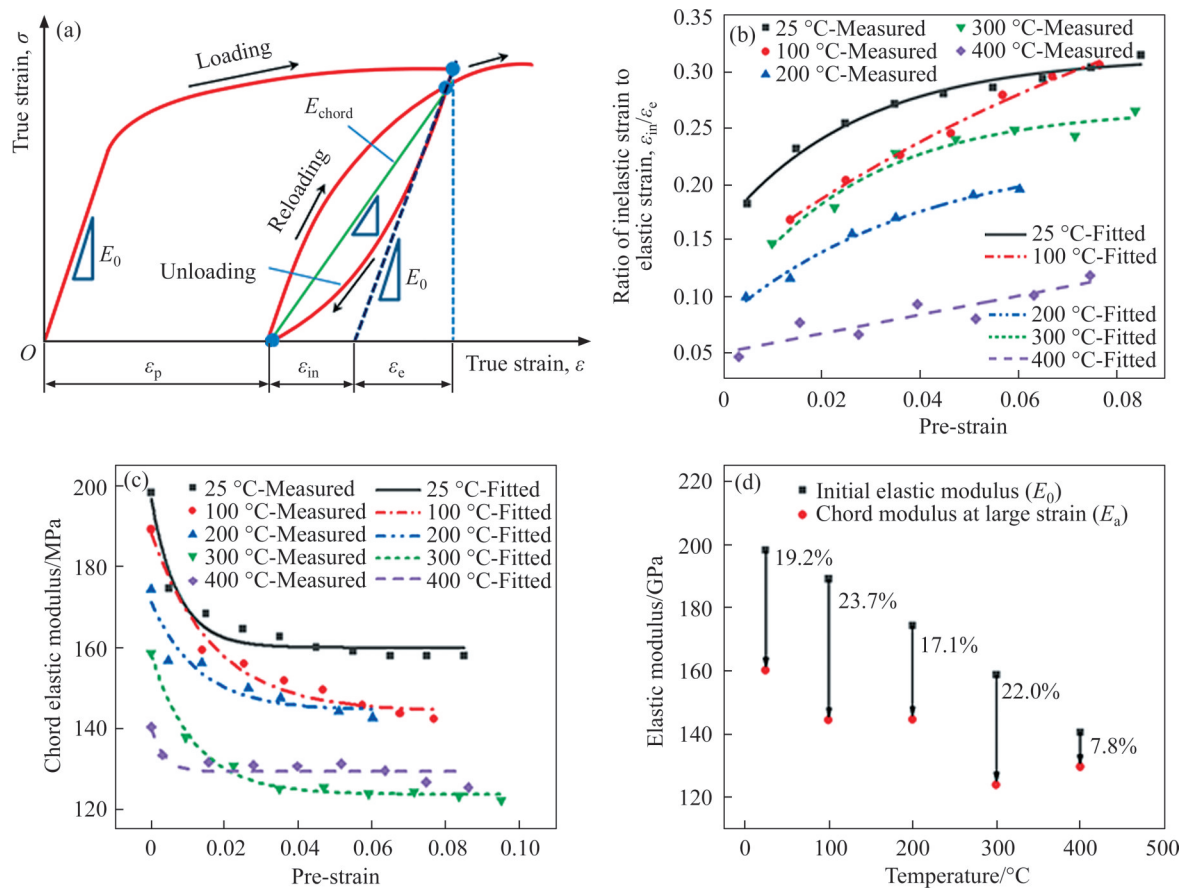


Figure 5 ULUR tests at various temperatures: (a) Schematic diagram of elastic modulus; (b) Ratio of inelastic modulus to elastic modulus as a function of pre-strain; (c) Chord elastic modulus as a function of pre-strain; (d) Deviation of initial elastic modulus and chord modulus at large strain

modulus exhibits significant temperature-dependent. The chord elastic modulus decreases as the pre-strain or temperature increases. However, the chord elastic modulus at $T=400\text{ }^{\circ}\text{C}$ is slightly higher than that at $T=300\text{ }^{\circ}\text{C}$, which may be caused by the temperature-induced texture evolution. The variation of chord modulus with pre-strain exhibits the same tendency as reported in Refs. [18–19], which is suitable for different materials.

Figure 5(d) shows the initial elastic modulus decreases with the increase of temperature. As demonstrated by YU [20], elastic modulus is a strength index of the inter-grain binding force that the decrease of initial elastic modulus is mainly due to the thermal softening of binding force among grains. Besides, the deviation between the initial elastic modulus E_0 and chord modulus E_a is also obtained. It can be found that the deviation value just fluctuates within the range of 17.1% to 23.7% when the temperature ranges from $25\text{ }^{\circ}\text{C}$ to $300\text{ }^{\circ}\text{C}$. However, the deviation of chord modulus is less than 10% when the temperature rises to $400\text{ }^{\circ}\text{C}$. This indicates that the temperature weakens the nonlinearity of chord elastic modulus E_{chord} . From the microscopic view, the variation of elastic

modulus is closely related to the microstructure evolution, textural change, thermal softening, and internal stress during cyclic elastoplastic deformation [20]. Especially, with the increase of temperature, the climb and annihilation process of dislocation will be enhanced. All these factors affect the attenuation of chord modulus in varying degrees at various temperatures. It is difficult to qualitatively analyze which factor is the most prominent.

3.1.3 Temperature dependence of Bauschinger effect

Bauschinger effect refers to the stress softening behavior of materials during reverse loading, and its strength difference also reflects the extent of nonlinear recovery. However, since it is difficult to determine the yield stress under reverse loading, many other methods for determining the Bauschinger effect have been reported, such as Bauschinger strain [21], Bauschinger stress [22], and Bauschinger energy [23].

To clarify the influence of the evolution of Bauschinger effect at elevated temperature on springback, the Bauschinger effect loop width (BELW) and Bauschinger effect loop area (BELA) were examined. Figures 6(a) and (b) illustrate the

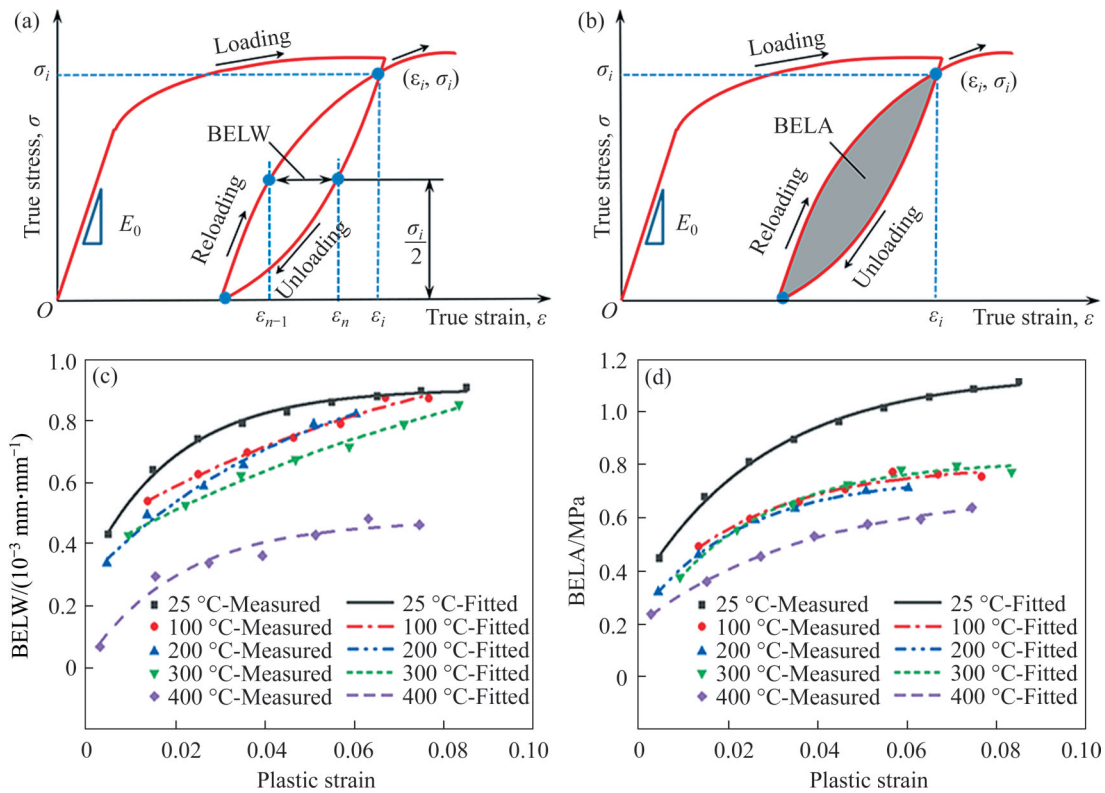


Figure 6 Uniaxial loading-unloading-reloading (ULUR) tests at various temperatures: (a) Schematic diagram of BELW; (b) Schematic diagram of BELA; (c) Relationship between BELW and the plastic strain; (d) Relationship between BELA and the plastic strain

characterization method of BELW and BELA [24]. The BELW is obtained by the strain difference at half of the maximum intersect stress between the unloading and reloading procedure. As for the BELA, it is obtained directly by calculating the area of the hysteresis loop, which represents the strain energy dissipation.

From Figures 6(c) and (d), the BELW and BELA exhibit strong thermal softening behavior, and the relationship between BELW (or BELA) and plastic strain shows an evolution law that grows exponentially and eventually becomes saturated.

In addition, Figure 7 presents that the relationship between BELW (or BELA) and inelastic strain is linear. The slope of the BELW or BELA represents the proportion of the Bauschinger effect to nonlinear recovery. If the value of the slope is equal to 1, it means that the Bauschinger effect dominates the nonlinear recovery completely.

According to Figure 7(a), the maximum value of the slope for BELW is only 0.62, which occurs

at $T=200\text{ }^{\circ}\text{C}$. Based on the values of the slope for BELW, the order is as follows: 200, 400, 25, 300 and $100\text{ }^{\circ}\text{C}$, while the deviation between the slope at $T=200\text{ }^{\circ}\text{C}$ and $400\text{ }^{\circ}\text{C}$ is very small. According to Figure 7(b), the slope for BELA at $T=25$ and $400\text{ }^{\circ}\text{C}$ is equal to 0.68. As a contrast, the minimum value of the slope for BELA is only 0.31, which occurs at $T=100\text{ }^{\circ}\text{C}$. In conclusion, the Bauschinger effect on the nonlinear recovery is weaker with a smaller slope. Furthermore, both BELW and BELA can reflect the Bauschinger effect, while BELA is preferable.

3.2 Springback behavior

3.2.1 Effect of temperature on springback

The springback parameters θ_1 , θ_2 and ρ defined in Figure 8(a) are determined. Under the condition without springback, the angles θ_1 and θ_2 , should be equal to 90° , and the sidewall curl radius ρ should be infinite. Figures (b) and (c) show the springback decreases with the increasing heating temperature as expected, which indicates that the elevated forming temperature can significantly reduce the springback angle of U-shape parts. However, there is no significant reduction of springback when the temperature exceeds $400\text{ }^{\circ}\text{C}$.

Figure 8(d) shows the measurement results of three springback parameters. For the angle θ_1 , the minimum springback angle of 97.78° occurs at $400\text{ }^{\circ}\text{C}$. Compared with cold forming, the springback angle is reduced by 9.78° . For the angle θ_2 , the springback occurs in the temperature range from $25\text{ }^{\circ}\text{C}$ to $300\text{ }^{\circ}\text{C}$, and the maximum springback angle is only 8.2° . However, the slight “spring-go” occurs after $300\text{ }^{\circ}\text{C}$ [25]. As for the sidewall curl radius ρ , which also increases with the increasing temperature, its value reaches nearly 1000 mm as the temperature exceeds $300\text{ }^{\circ}\text{C}$, and the sidewall can be regarded as a straight wall under this condition, suggesting that the sidewall curl springback is greatly weakened at elevated temperature. According to the above analysis, it indicates that the bending angular springback can be reduced by 8° to 10° , and the sidewall curl springback can be eliminated via heating the sheet to proper temperature for non-isothermal forming.

3.2.2 Effects of hardness and microstructure on springback

The Vickers hardness along the U-shape profile

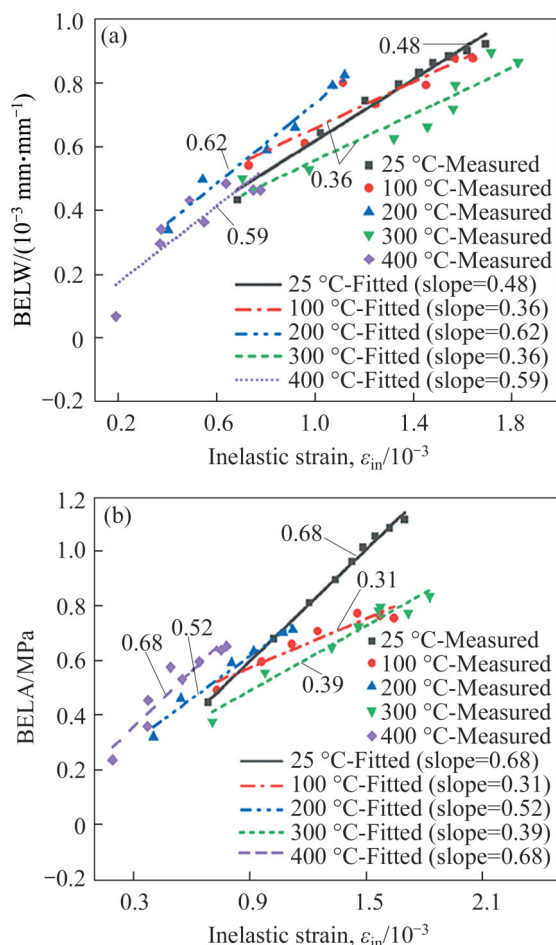


Figure 7 Relationship between (a) BELW and inelastic strain and (b) BELA and inelastic strain

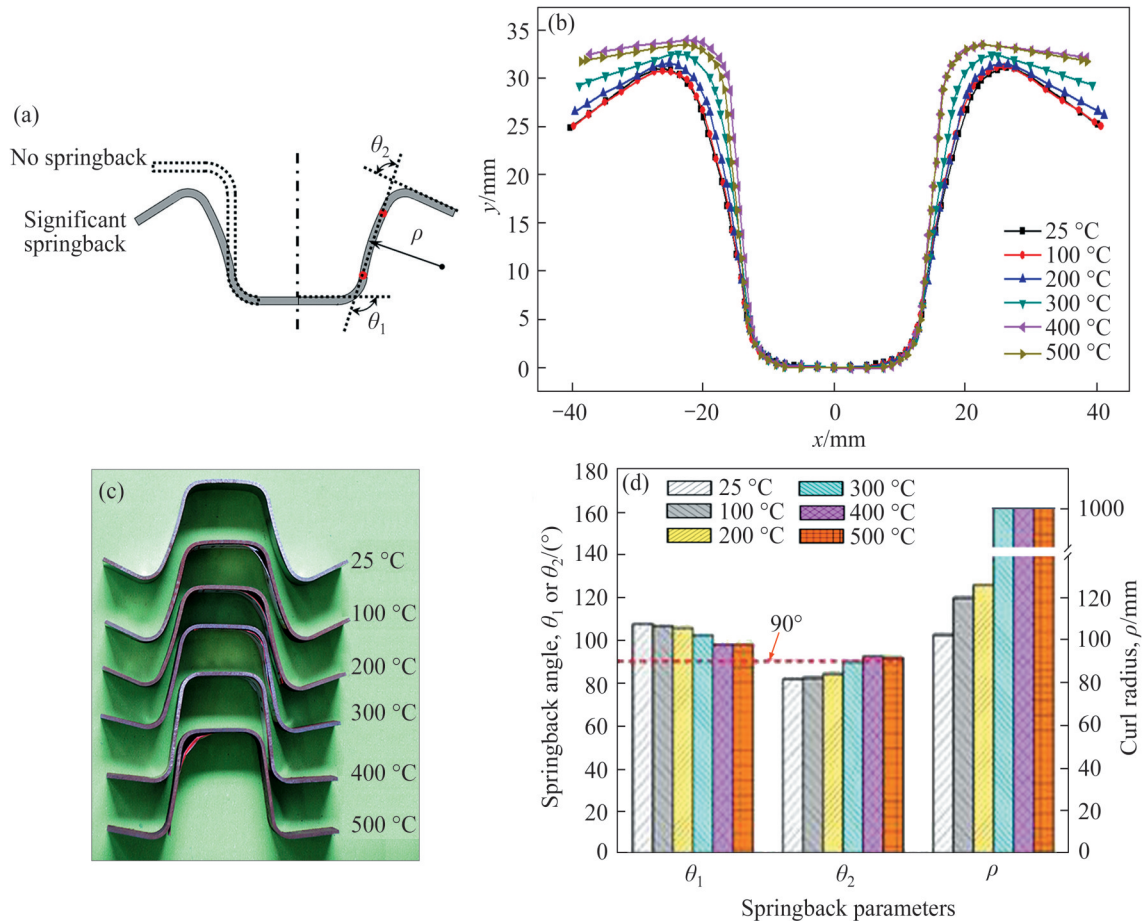


Figure 8 (a) Springback parameters; (b) Section profile; (c) U-shape parts at various heating temperatures; (d) Bending angular springback and sidewall curl radius of U-shape parts at different heating temperatures

shown in Figure 9(a) was measured at a load of 3.0 N. The relationship between Vickers hardness and temperature at different positions are illustrated in Figure 9(b). With the increasing heating temperature of the blank sheet, the overall Vickers hardness firstly increases and then decreases. The Vickers hardness at $T=200\text{ }^{\circ}\text{C}$, $300\text{ }^{\circ}\text{C}$ and $400\text{ }^{\circ}\text{C}$ is greater than HV 300, which is only slightly lower than that at $T=25\text{ }^{\circ}\text{C}$. This indicates that the DP980 steel sheet is suitable for warm forming since it can maintain a relatively high strength after deformation. The hardness of position-O without deformation is almost the lowest among all the positions. The Vickers hardness at the other positions which experience stretching, bending, and reverse bending process is higher, especially at positions-C and -D. These results indicate that complicated loading or forming temperature can affect the hardness significantly. The difference in hardness of the U-shape parts is mainly due to the

carbon precipitation induced by plastic deformation or tempering [26].

The different carbon contents also reflect the martensite size effect. WANG et al [27] have pointed out that the deformation of fine martensite laths is more uniform compared to coarse martensite lath. As shown in Figure 10, the microstructures at position-C of the U-shape parts at different heating temperatures are examined. It is shown that the martensite size at $T=100\text{ }^{\circ}\text{C}$ and $200\text{ }^{\circ}\text{C}$ is coarser than that at the other temperatures, and the martensite size is finer with the increasing heating temperature after $T=200\text{ }^{\circ}\text{C}$.

To examine the effect of microstructure heterogeneity on the springback, the martensitic area fraction at various temperatures is calculated quantitatively and shown in Figure 9(c). It can be found that the martensitic area fraction along the section profile of U-shape parts varies significantly at different temperatures. The deviations of

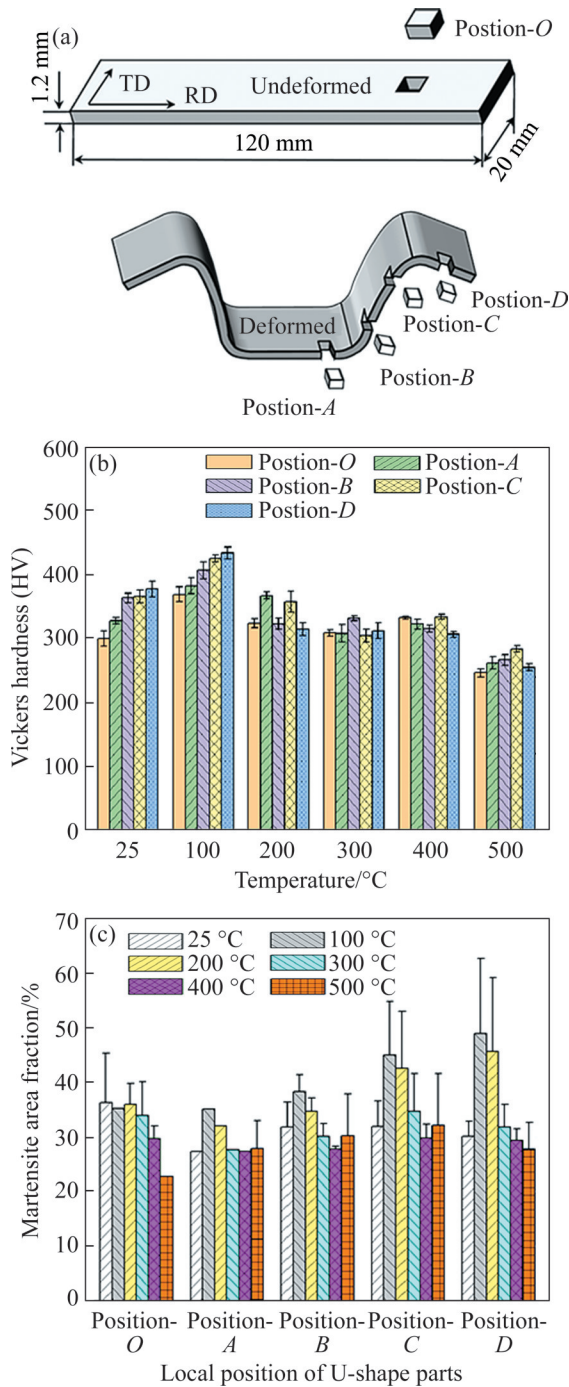


Figure 9 (a) Schematic diagram of sampling; (b) Vickers hardness; (c) Martensite area fraction of sheet metal before and after warming forming

martensitic area fraction are large in the temperature range from 25 °C to 200 °C, which may be caused by the coarse martensite laths. As a contrast, the deviation of martensitic area fraction at 400 °C is the minimum. It is worth to mention that the U-shape part heated at 400 °C also has the smallest springback angular and curl radius. Therefore, it could be concluded that a suitable heating

temperature can improve the microstructure uniformity and reduce the springback effectively.

4 Conclusions

In this paper, the principle of springback reduction during warm forming of dual-phase steel is clarified by revealing the temperature dependence of relevant mechanical parameters. The research findings can provide basis data for the finite element prediction of springback in the warm forming process. The main conclusions are as following:

1) The monotonic stress–strain response in the temperature range from 100 °C to 350 °C has no obvious thermal-softening effect, while a slight dynamic strain aging effect exists, which also affects the initial elastic modulus. Furthermore, the flow stress at a warm temperature is lower than that at room temperature.

2) As the heating temperature of the DP980 steel sheets increases and the plastic strain accumulates, the weight of the nonlinear elastic recovery in the total recovery decreases, and the chord modulus is also reduced, indicating that the springback is gradually dominated by linear elastic recovery.

3) The Bauschinger effect of DP980 steel sheets is weakened at elevated temperature, while there is a slight rebound in the temperature range from 100 °C to 300 °C. Furthermore, a linear relationship between the Bauschinger effect and inelastic strain is also observed.

4) The martensite size effect of dual-phase steel and its uneven distributions are also one of the key factors which lead to springback during warm forming. The microstructure morphology can be effectively homogenized by choosing a suitable forming temperature, and the purpose of reducing springback can be achieved.

Contributors

The overarching research goals were developed by LIN Qi-quan, WANG Zhen-zhu, DONG Wen-zheng. WANG Zhen-zhu performed the data analysis and wrote the manuscript. DONG Wen-zheng helped perform the analysis with experimental results and revised the manuscript. BU Gen and HUANG Jin-san participated in the ULUR test at elevated temperatures.

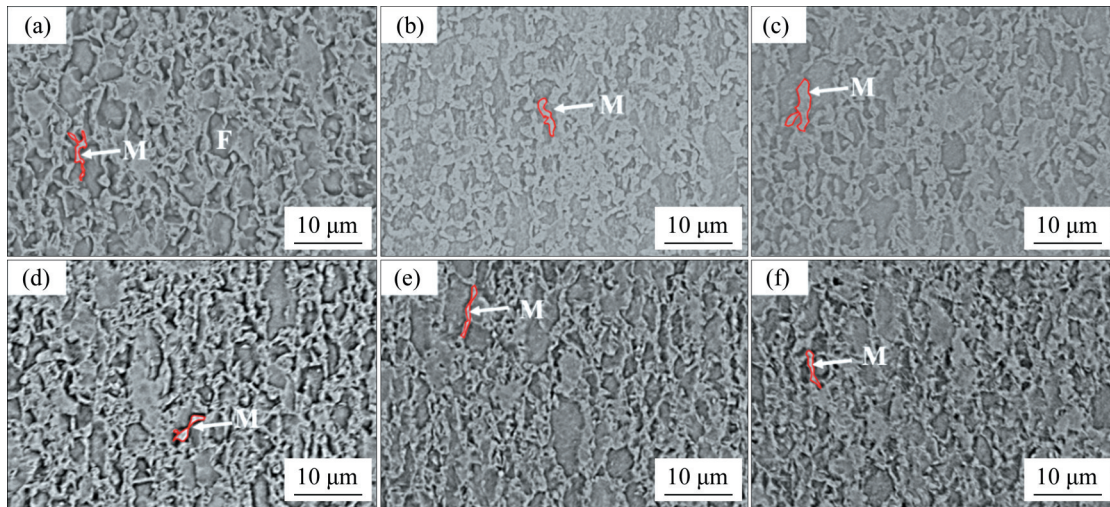


Figure 10 Microstructural change of position-C at the heating temperature of (a) 25 °C, (b) 100 °C, (c) 200 °C, (d) 300 °C, (e) 400 °C, and (f) 500 °C after U-draw bending test (M: martensite; F: ferrite)

Conflict of interest

LIN Qi-quan, WANG Zhen-zhu, DONG Wen-zheng, BU Gen, and HUANG Jin-shan declare that they have no conflict of interest.

References

- [1] WANG Z G, YOSHIKAWA Y, OSAKADA K. A new forming method of solid bosses on a cup made by deep drawing [J]. *CIRP Annals*, 2013, 62(1): 291–294. DOI: 10.1016/j.cirp.2013.03.057.
- [2] WANG Z G, HIRASAWA K, YOSHIKAWA Y, et al. Forming of light-weight gear wheel by plate forging [J]. *CIRP Annals*, 2016, 65(1): 293–296. DOI: 10.1016/j.cirp.2016.04.134.
- [3] YANG Xiao-ming, DANG Li-ming, WANG Yao-qi, et al. Springback prediction of TC4 titanium alloy V-bending under hot stamping condition [J]. *Journal of Central South University*, 2020, 27(9): 2578–2591. DOI: 10.1007/s11771-020-4483-y.
- [4] MA Wei-ping, WANG Bao-yu, XIAO Wen-chao, et al. Springback analysis of 6016 aluminum alloy sheet in hot V-shape stamping [J]. *Journal of Central South University*, 2019, 26(3): 524–535. DOI: 10.1007/s11771-019-4024-8.
- [5] MORI K, BARIANI P F, BEHRENS B A, et al. Hot stamping of ultra-high strength steel parts [J]. *CIRP Annals*, 2017, 66(2): 755–777. DOI: 10.1016/j.cirp.2017.05.007.
- [6] LEE E H, HWANG J S, LEE C W, et al. A local heating method by near-infrared rays for forming of non-quenchable advanced high-strength steels [J]. *Journal of Materials Processing Technology*, 2014, 214(4): 784–793. DOI: 10.1016/j.jmatprotec.2013.11.023.
- [7] SAITO N, FUKAHORI M, MINOTE T, et al. Elasto-viscoplastic behavior of 980 MPa nano-precipitation strengthened steel sheet at elevated temperatures and springback in warm bending [J]. *International Journal of Mechanical Sciences*, 2018, 146–147: 571–582. DOI: 10.1016/j.ijmecsci.2017.11.044.
- [8] OZTURK F, TOROS S, KILIC S. Tensile and spring-back behavior of DP600 advanced high strength steel at warm temperatures [J]. *Journal of Iron and Steel Research, International*, 2009, 16(6): 41–46. DOI: 10.1016/S1006-706X(10)60025-8.
- [9] KAYHAN E, KAFTANOGLU B. Experimental investigation of non-isothermal deep drawing of DP600 steel [J]. *The International Journal of Advanced Manufacturing Technology*, 2018, 99(1–4): 695–706. DOI: 10.1007/s00170-018-2403-1.
- [10] MORI K, MAKI S, TANAKA Y. Warm and hot stamping of ultra high tensile strength steel sheets using resistance heating [J]. *CIRP Annals*, 2005, 54(1): 209–212. DOI: 10.1016/S0007-8506(07)60085-7.
- [11] NGUYEN N T, SEO O, LEE C, et al. Mechanical behavior of AZ31B Mg alloy sheets under monotonic and cyclic loadings at room and moderately elevated temperatures [J]. *Materials*, 2014, 7(2): 1271–1295. DOI: 10.3390/ma7021271.
- [12] ZANG Shun-lai, LEE M G, SUN Li, et al. Measurement of the Bauschinger behavior of sheet metals by three-point bending springback test with pre-strained strips [J]. *International Journal of Plasticity*, 2014, 59: 84–107. DOI: 10.1016/j.ijplas.2014.03.015.
- [13] WANG Chuan-tao, KINZEL G, ALTAN T. Mathematical modeling of plane-strain bending of sheet and plate [J]. *Journal of Materials Processing Technology*, 1993, 39(3–4): 279–304. DOI: 10.1016/0924-0136(93)90164-2.
- [14] CAI Zheng-yang, WAN Min, LIU Zhi-gang, et al. Thermal-mechanical behaviors of dual-phase steel sheet under warm-forming conditions [J]. *International Journal of Mechanical Sciences*, 2017, 126: 79–94. DOI: 10.1016/j.ijmecsci.2017.03.009.
- [15] XUE Xin, LIAO Juan, VINCZE G, et al. Experimental assessment of nonlinear elastic behaviour of dual-phase steels and application to springback prediction [J].

- International Journal of Mechanical Sciences, 2016, 117: 1–15. DOI: 10.1016/j.ijmecsci.2016.08.003.
- [16] SUN Li, WAGONER R H. Complex unloading behavior: Nature of the deformation and its consistent constitutive representation [J]. International Journal of Plasticity, 2011, 27(7): 1126–1144. DOI: 10.1016/j.ijplas.2010.12.003.
- [17] QUEIROZ R R U, CUNHA F G G, GONZALEZ B M. Study of dynamic strain aging in dual phase steel [J]. Materials Science and Engineering A, 2012, 543: 84–87. DOI: 10.1016/j.msea.2012.02.050.
- [18] MORESTIN F, BOIVIN M. On the necessity of taking into account the variation in the Young modulus with plastic strain in elastic-plastic software [J]. Nuclear Engineering and Design, 1996, 162(1): 107–116. DOI: 10.1016/0029-5493(95)01123-4.
- [19] YOSHIDA F, UEMORI T, FUJIWARA K. Elastic-plastic behavior of steel sheets under in-plane cyclic tension-compression at large strain [J]. International Journal of Plasticity, 2002, 18(5–6): 633–659. DOI: 10.1016/S0749-6419(01)00049-3.
- [20] YU Hai-yan. Variation of elastic modulus during plastic deformation and its influence on springback [J]. Materials & Design, 2009, 30(3): 846–850. DOI: 10.1016/j.matdes.2008.05.064.
- [21] WOOLLEY R L. LXIV. The Bauschinger effect in some face-centred and body-centred cubic metals [J]. The London, Edinburgh, and Dublin Philosophical Magazine and Journal of Science, 1953, 44(353): 597–618. DOI: 10.1080/14786440608521038.
- [22] MOAN G D, EMBURY J D. A study of the bauschinger effect in Al–Cu alloys [J]. Acta Metallurgica, 1979, 27(5): 903–914. DOI: 10.1016/0001-6160(79)90125-1.
- [23] TITCHENER A L, BEVER M B. The stored energy of cold work [J]. Progress in Metal Physics, 1958, 7: 247–338. DOI: 10.1016/0502-8205(58)90006-6.
- [24] MA Hong-wei, WANG Zhi-rui. The influence of the bauschinger effect on springback prediction for dual phase steel [C]// SAE Technical Paper Series. 400 Commonwealth Drive, Warrendale, PA, United States: SAE International, 2006, 5(115): 181–187. DOI: 10.4271/2006-01-0145.
- [25] KOMGRIT L, HAMASAKI H, HINO R, et al. Elimination of springback of high-strength steel sheet by using additional bending with counter punch [J]. Journal of Materials Processing Technology, 2016, 229: 199–206. DOI: 10.1016/j.jmatprotec.2015.08.029.
- [26] GALINDO-NAVA E I, RIVERA-DÍAZ-DEL-CASTILLO P E J. Understanding the factors controlling the hardness in martensitic steels [J]. Scripta Materialia, 2016, 110: 96–100. DOI: 10.1016/j.scriptamat.2015.08.010.
- [27] WANG M M, HELL J C, TASAN C C. Martensite size effects on damage in quenching and partitioning steels [J]. Scripta Materialia, 2017, 138: 1–5. DOI: 10.1016/j.scriptamat.2017.05.021.

(Edited by ZHENG Yu-tong)

中文导读

温热成形下双相钢板热-力学性能与回弹行为

摘要: 对于不可淬火的双相钢(DP钢), 温热成形技术可以显著降低其回弹量, 引起其弹性和非弹性回复降低的力学参数与温度有强烈的相关性, 尤其是在循环变形条件下。本文对DP980钢板在25~500 °C温度下进行了单轴加载和循环加载-卸载试验, 研究温度相关流变应力、非线性弹性回复和包辛格效应的演化规律。结果表明, DP980钢板的弹性模量和包辛格效应均随预应变的增大而呈指数型演化, 并随成形温度的升高而减小。由于动态应变时效效应的影响, 该演化行为会出现反弹现象。同时, 在不同温度下, 包辛格效应与非弹性应变呈线性关系演化, 且包辛格效应在总应变中的权重随着温度的升高而降低, 说明在较高的温度下回弹逐渐以线弹性回复为主。此外, 还进行了U形拉深-弯曲的工艺试验, 以阐明维氏硬度分布和马氏体尺寸效应对回弹行为的影响。

关键词: 温热成形; 双相钢板; 回弹行为; 非线性弹性回复; 包辛格效应